Grain size fractionation by process-driven sorting in sandy to muddy deltas

van der Vegt, Helena; Storms, Joep E.A.; Walstra, Dirk Jan R.; Nordahl, Kjetil; Howes, Nick C.; Martinius, Allard W.

DOI
10.1002/dep2.85

Publication date
2020

Document Version
Final published version

Published in
Depositional Record

Citation (APA)
van der Vegt, H., Storms, J. E. A., Walstra, D. J. R., Nordahl, K., Howes, N. C., & Martinius, A. W. (2020). Grain size fractionation by process-driven sorting in sandy to muddy deltas. *Depositional Record*, *6*(1), 217-235. https://doi.org/10.1002/dep2.85

Received: 29 January 2019 | Revised: 16 June 2019 | Accepted: 29 June 2019

DOI: 10.1002/dep2.85

ORIGINAL RESEARCH ARTICLE

The Depositional Record Open Access
A journal of the International Association of Sedimentologists
WILEY

Grain size fractionation by process-driven sorting in sandy to muddy deltas

Helena van der Vegt[1,2] | **Joep E.A. Storms**[1] | **Dirk-Jan R. Walstra**[2] | **Kjetil Nordahl**[3] | **Nick C. Howes**[4] | **Allard W. Martinius**[1,3]

[1]Department of Geoscience and Engineering, Delft University of Technology, Delft, The Netherlands

[2]Deltares, Delft, The Netherlands

[3]Equinor, Trondheim, Norway

[4]MathWorks, Natick, Massachusetts

Correspondence
Helena van der Vegt, Deltares, Delft, The Netherlands.
Email: helena.vandervegt@deltares.nl

Abstract

Modern and ancient analogues are often consulted by geologists to help understand subsurface systems. While modern analogues provide information on the areal relationship between facies, ancient systems provide detailed data on the vertical facies variations, typically along a two-dimensional outcrop. Combining data from modern and ancient systems effectively requires translating areal morphology, which is often still evolving, to the related sediments preserved in three dimensions. Process-based models simulate both depositional processes while preserving stratigraphy. These models can be employed to unravel the relationship between sediment supply and preserved deposits in natural systems and to help integrate field data. Four synthetic deltas were modelled using different sediment supply compositions, from coarse to very fine sand systems. The resultant sedimentary deposits are classified into architectural elements, and the grain size composition of each architectural element is studied over time. Facies that are extensive in their horizontal dimensions are often less abundant in three-dimensional preserved deposits. Between deltas, grain size compositions of a specific architectural element type (e.g. mouth bars) are more similar than their corresponding sediment supply compositions. This is due to selective deposition of grain size classes across each architectural element type. This selective deposition causes overrepresentation of the same range of grain sizes, even for systems with different sediment supply compositions. When a particular supply composition does not contain enough of the overrepresented grain size class for a particular architectural element, that element will be under-supplied and constitute a smaller proportion of the overall delta deposits. It is imperative to account for overrepresentation of grain size classes in particular architectural elements when estimating palaeo-sediment supply, delta architecture and morphology from field data. Even when data availability/accessibility does not allow the inclusion of distal deposits in field studies, process-based simulations can contribute valuable information on sediment sorting patterns in three dimensions.

KEYWORDS

Grain size, mouth bar, river delta architecture, sorting

1 | INTRODUCTION

Source-to-sink studies examine basin-scale partitioning and preservation of sediment through time. Such studies are still largely volume-based, but new work is deciphering the grain size distribution across the system (Michael *et al.*, 2014; Helland-Hansen *et al.*, 2016; Allen, 2017). Numerical models simulating the transport of sediment along parts of the source-to-sink trajectory can help to understand the distribution of different grain sizes within the geological record.

At the scale of an individual depositional environment such as a delta, morphology and stratigraphy are known to be influenced by the characteristics of the supplied sediment (Orton and Reading, 1993). Classifications of deltas by grain size composition is taken to refer to the mixture of all sediment arriving at the delta. Based on this supplied sediment composition, a number of morphological and stratigraphic traits can be inferred, such as shoreline shape, number of channels active at the same time, rate of channel migration and channel width and depth (Orton and Reading, 1993; Caldwell and Edmonds, 2014; Burpee *et al.*, 2015; van der Vegt *et al.*, 2016).

However, a discrepancy exists between descriptions of modern and ancient deltaic systems in the scientific literature with an apparent bias towards fine sand deltas from the ancient rock records (Table 1). Where modern deltas are classified by their fluvially supplied sediment composition or delta top grain sizes (Syvitski and Farrow, 1989; Orton and Reading, 1993; Syvitski and Saito, 2007), ancient examples from outcrop or subsurface are studied based on preserved and accessible deposits. It has previously been noted that field studies seldom include detailed study of distal, muddier (prodelta) deposits, instead focussing on proximal, sandier deposits (Bhattacharya and MacEachern, 2009). In addition, modern systems are often studied using plan-view, remote sensing images, while outcrop and subsurface studies focus on vertical profiles.

Sediment grain size fractionation is known to occur within the delta environment, causing different mixtures of grain sizes to settle preferentially at different locations across the delta (Wright, 1977; Jerolmack and Paola, 2010). The influence of process-driven sediment fractionation on the relationship between plan view observations of modern deltas and vertical observations of delta architecture is investigated here. To accomplish this deposited sediment is classified into six distinct architectural elements: channel accretion (channel bars), channel fill, delta top background (overbank) sedimentation, mouth bars, delta front background sedimentation and prodelta.

One of the most important identifying features of ancient deltaic deposits are the sandy clinoforms of their delta front mouth bar complexes (Forzoni *et al.*, 2015) and mouth bar complexes are therefore of particular interest in the analysis. Mouth bars form in the highly complex transitional region influenced by both fluvial and marine forces. Hydrodynamically, a mouth bar develops when sediment-laden jets exit a channel mouth into a body of standing water. The jets spread out and decelerate, whereby sediment settles out of the water column. Wright (1977) was one of the first to describe mouth bar deposition in terms of inertial, frictional and buoyant forces, in addition to reworking forces (tides, waves). More recently, the detailed morphodynamic mechanisms of the formation of individual mouth bars have been investigated using numerical simulations in Delft3D (Edmonds and Slingerland, 2007; Geleynse *et al.*, 2010; Esposito *et al*, 2013; Mariotti *et al.*, 2013; Canestrelli *et al.*, 2014). Some studies have also focused on the influence of various external parameters on these mouth bars such as discharge, waves, tides and basin slope (Leonardi *et al.*, 2013; Jimenez-Robles *et al.*, 2016; Gao *et al.*, 2019).

This paper investigates how the upstream sediment supply composition is translated not only to the mouth bars, but across the whole range of architectural elements. While the complete proximal to distal delta transect may not be preserved or accessible in the geological record, numerical

TABLE 1 Ancient and modern deltas from the literature, classified by grain size (Orton and Reading, 1993; Syvitski and Saito, 2007; Howell *et al.*, 2008; Hubbard *et al.*, 2010; Ainsworth *et al.*, 2016). Literature on ancient deltas show a bias for describing fine sand deltas

Grain size	Gravel/coarse-grained deltas	Very fine to medium sand deltas	Mud/Silt deltas
Modern deltas	Punta Gorda(NI), Waipaoa (NZ), Yallahs (JM), Alta (NO), Bella Coola (CA), Colville (US), Homanthko (CA), Klinaklini (CA), Noeick (CA)	Burdekin (AU), Shaolhaven (AU), Copper (US), Ebro (ES), Mackenzie (CA), Fraser (CA), Squamish (CA), Klang (MY), Mahakam (ID), Mekong (VN), Niger (NG), Po (IT), Tiber (IT), Rhone (FR), Sao Francisco (BR)	Amazon (BR), Ganges-Brahmaputra (IN), Huange/Yellow (CN), Irrawady (MM), Mississippi (USA), Ord (AU), Orinoco (VE), Yangtze (CN)
Ancient deltas	Dorotea Formation (Magallanes Basin, Chile)	Ferron Sandstone Mbr (Mancos Shale), Panther Tongue (Star Point Sandstone), Spring Canyon Mbr, Kenilworth Mbr, Sunnyside Mbr, Grassy Mbr (Blackhawk Fm), John Henry Mbr (Straight Cliffs Fm) (Mesaverde Group, Utah, USA), Drumheller Mbr (Horseshoe Canyon Fm, Canada), Rannoch Fm, Ness Fm (Brent Group, North Sea)	?

models like Delft3D provide three-dimensional depositional data, over time, in the context of known (user defined) boundary conditions. Therefore the use of numerical models is particularly suited to study the effect of palaeo-sediment supply composition on preserved deltaic deposits. The advantage is that the numerical simulations provide information on the hydrodynamic conditions, sediment deposition and preserved deposits, thereby linking hydrodynamic data and sedimentary deposits in three dimensions (Figure 1). The analyses presented here show how sediment sorting and grain-size fractionation across a delta environment could bias the interpretation of the deltaic deposits towards sandy deltas, reported to dominate ancient deltaic deposits (Bhattacharya and MacEachern, 2009).

2 | METHODOLOGY FOR CREATING AND CLASSIFYING 4D SYNTHETIC DELTA ANALOGUES

Process-based models like Delft3D (Lesser *et al.*, 2004) provides a well-established methodology to investigate the

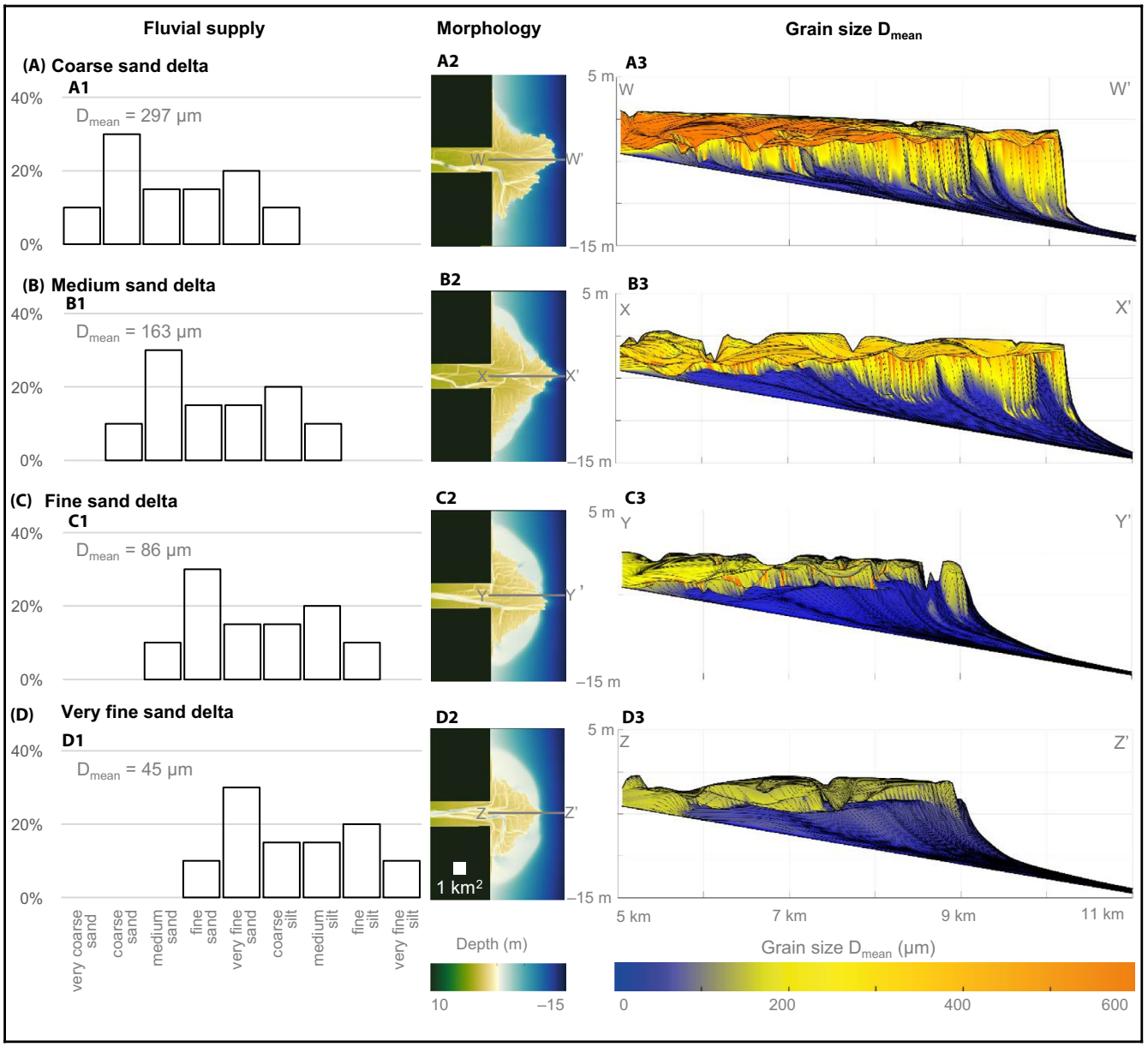

FIGURE 1 The fluvial sediment supply composition is shown for each of the four deltas (A1, B1, C1, D1), including the geometric mean of the supply composition, the final bathymetry of the resultant delta (A2, B2, C2, D2) and a representative cross section showing time lines and geometric mean of the grain size distributions within the delta (A3, B3, C3, D3). Note that the vertical exaggeration in the delta cross sections amounts to 100. The grain sizes associated with the supplied sediment classes are very coarse sand = 1,000 µm, coarse sand = 750 µm, medium sand = 375 µm, fine sand = 200 µm, very fine sand = 100 µm, coarse silt = 62 µm, medium silt = 31 µm, fine silt = 16 µm, very fine silt = 8 µm

effects of specific parameters on deltaic morphology (Storms *et al.*, 2007; Edmonds and Slingerland, 2009; Geleynse *et al.*, 2010; Caldwell and Edmonds, 2014; Burpee *et al.*, 2015), but applying these models to study detailed three-dimensional grain size distributions still provides a virtually unexplored research avenue. Using Delft3D to produce four-dimensional (three spatial dimensions and time) synthetic stratigraphic architecture of deltas allows the study of evolving and preserved deposits over time.

Four deltas were simulated in Delft3D using four unique, bimodal, compositions for the supplied sediment, containing different proportions of very fine silt up to very coarse sand classes (Figure 1A1, B1, C1, D1). In natural systems, bimodal grain size distributions in deltaic sediment supply are the result of two dominating transport mechanisms, bed load and suspended load transport, which control sediment delivery along the catchment and fluvial system towards the delta (Orton and Reading, 1993; Syvitski and Saito, 2007). The overall supply composition in any system strongly depends on area, relief, and climate regime of the catchment and fluvial domain (Bhattacharya *et al.*, 2016).

In the models described here, the supplied sediment concentration is the same for all simulations and does not change with time. For all models, the imposed discharge is large enough to mobilize all the grain size fractions in the supply mixtures at the fluvial boundary. However, the rate at which sediment classes traverse the model's fluvial domain to reach the area of interest (the basin) is dependent not only on whether any specific gain size class is mobilized. The sediment mixture available locally within the bed, the concentration and settling velocity of entrained sediment as well as the local water depth, slope and flow velocities also control the transport of the different sediment fractions. The local responses to the changing velocity map across the delta are therefore highly variable across the model domain. For sediment mixtures of larger grain size classes, a larger proportion of the sediment mass travels as bedload rather than suspended load. In addition, coarser sediments also have larger settling velocities. For these reasons, if discharge and sediment concentration were the same for all four simulated deltas, the coarser-grained systems would prograde much slower than the fine-grained systems. Larger flow velocities were imposed for coarser-grained simulations to accelerate their transport of sediment to the basin. All discharge values fall within the range reported in natural systems (Milliman and Syvitski, 1992) with the very-fine sand delta receiving the smallest discharge (1,200 m^3/s) while the coarse sand delta receives the largest (1,800 m^3/s). This means that the rate at which sediment is supplied to each delta is different. For comparison, the discharge imposed at the start of the simulation, the initial bathymetry at the boundary and the geometric D_{mean} of the supply composition have been used to calculate a Shields number associated with the discharge for each simulation (Table 2). Due to the use of the Manning roughness coefficient, the shields number will vary with water depth in the sloped basin. The values at 4 m water depth were calculated, as this is the water depth at the discharge boundary at the start of the simulation.

The time-constant discharge mimics a constant state of bank full discharge, and together with Delft3D's morphological scaling factor (MORFAC = 30) the simulations represent prograding deltas on a multi-century to millennial temporal scale (Li *et al.*, 2017). Delta development is mature enough by the end of the simulations to encapsulate all relevant dynamics. The simulations consist of a fluvial channel debouching into a sloped basin (0.1°). The marine reworking processes in all models are the same and consists of a semi-diurnal tide (1 m amplitude) and waves (amplitude of 0.2 m, period of 3 s) arriving perpendicular to the shoreline. It was found that in order to simulate sediment distributions similar to that found in natural systems using Delft3D, at least some small wave activity is required in the basin in order to stir up the smaller-grained sediment classes deposited in the basin, as would be the case in any active coastal system.

Using a combination of hydrodynamic, morphological and sedimentary data, a new algorithm was created to classify deposited sediment into the following architectural elements: channel accretion (channel bars), channel fill, delta top background (overbank), mouth bar, delta front

TABLE 2 A characteristic Shields number calculated for the discharge boundary and the channel identification cut-off velocity

Model	Geometric D_{mean} (μm)	Shields number discharge	Shields number channel recognition
Coarse sand delta	297	0.599	1.048
Medium sand delta	163	0.863	1.752
Fine sand delta	86	1.251	2.452
Very fine sand delta	45	1.906	2.530

The calculations are based on the geometric mean grain size of the supplied sediment compositions, the velocity corresponding to the discharge boundary and initial bathymetry or the cut-off velocity for channel recognition, and because the simulations use the Manning roughness coefficient, the calculations assume a depth of 4 m, which is the initial water depth at the discharge boundary. These are only indicative numbers, as local velocities, grain size compositions and water depth can vary greatly both spatially and in time.

background and prodelta. Examples of plan view classification are shown in Figures 2B through 5B. The active channel network is responsible for distributing the supplied sediment across the delta and is therefore the most important factor controlling the three-dimensional shape of a delta (Syvitski *et al.*, 2005). Identifying the active channel network for each output time interval is then the first step in classifying the architectural elements. To identify active channels, a cut-off value is assigned for flow velocity, whereby a cell with a larger flow velocity than the cut-off value is defined to form part of the active channel network. The cut-off velocities used in the simulations fall between 1.19 and 0.62 m/s, and are specified for each simulation. It has not yet been possible to identify an efficient algorithm for determining these cut-off values in an automated fashion, and this is surely a topic that requires further investigation. Therefore, the value selection was done heuristically based on inspection of the channel networks delivered by different velocity cut-off values. When the value is too low, the identified channel network contracts and does not include the distal sections of the channel network as seen in the bathymetry plots. However, when the cut-off value is too large the identified network spills over the sides of the channel features visible in the bathymetry and also becomes diffuse at the mouths of the channels, incorporating the mouth bar deposits into the identified channel network. The criterion for selecting the best cut-off value was a value which minimizes these observed errors in network identification. The selected velocity cut-off values were also expressed as Shields numbers for each of the simulations for comparison to the input parameters (Table 2). The results are independent of the selected discharge values and channel velocity cut-off values (see Appendix 1).

The next cut-off value to be defined is the elevation at which the delta brink point occurs, which is the depth value separating the delta top and the delta front. A unique delta brink point is defined for each output time interval in each simulation by radially averaging the overall delta bathymetry for each time interval and then identifying the depth at which there is a break in gradient (van der Vegt *et al.*, 2016).

Based on the identified active channel network and the delta brink point, the architectural elements are assigned. The channel accretion classification is assigned to deposition occurring within the active channel network, or in an element which was part of the active channel network in the previous output interval (i.e. where the channel network was in the process of deactivating). Channel fill deposits accumulate in previously active channel network cells, until the delta brink point elevation is reached. Any sediment depositing above the delta brink point is assigned the classification of delta top background sedimentation, which incorporates delta plain and overbank deposition. Mouth bars consist of rapidly depositing (more than 0.3 m of deposition during one output time interval) sediment in proximity to active channel mouths (within 200 m). In the definition employed here mouth bars can only deposit below the delta brink elevation and above wave base (4 m in this case). The remainder of the deposition is separated into delta front background sedimentation (between the delta brink point and wave base) and prodelta (below wave base). To form part of the active delta deposition, a cell has to show at least 15 mm of deposition in one output time interval. Once this threshold is reached, any further deposition at this location is taken to contribute to the active delta deposition.

The classification was performed for deposits in each of the 320 output intervals, as well as for the final preserved deposits. This allows the study of not only the preserved deposits but also the intermediate deposits developed during delta progradation. As with all classifications, whether in modelling, experimental or field studies, classification requires the definitions of cut-off values which divide naturally grading distributions into distinct categories. Resultant classes may not be fully generic, but within the parameter space considered here they are consistent and therefore useful for comparisons. A more detailed description of the classification process is available in appendix I of van der Vegt (2018).

3 | RESULTS OF SEDIMENT FRACTIONATION ACROSS THE DELTA

The largest areas are spanned by the delta top background, the delta front background and the prodelta deposits, while the channel accretion, channel fill and mouth bar deposits cover only a small proportion of the delta area at any one time (Figures 2B, 3B, 4B and 5B). While the delta front background area increases from coarse sand to very fine sand delta, the delta top background area becomes correspondingly smaller.

In the coarse sand delta (Figure 2C and D), the two coarsest sand fractions (coarse and very coarse sand) are deposited mainly in the active channels. The medium and fine sand fractions (Figure 2E and F) also deposit within the channels, but in addition spread out more diffusely at the channel mouths. In the other delta models, the two coarsest grain size fractions in the supplied sediment also deposit in the active channel locations (Figures 3C,D,E, 4C,D and 5C,D). However, since the medium to very fine sand deltas are supplied with little to no coarse and very coarse sand, and since the medium, fine and very fine sand fractions not only deposit in the active channel network, but also spread out adjacent to the channels, it becomes difficult to distinguish the active channels from the surrounding deposits by merely looking at the grain size class maps. It is even more difficult to distinguish the depositional composition of the mouth bar deposits in the plan view

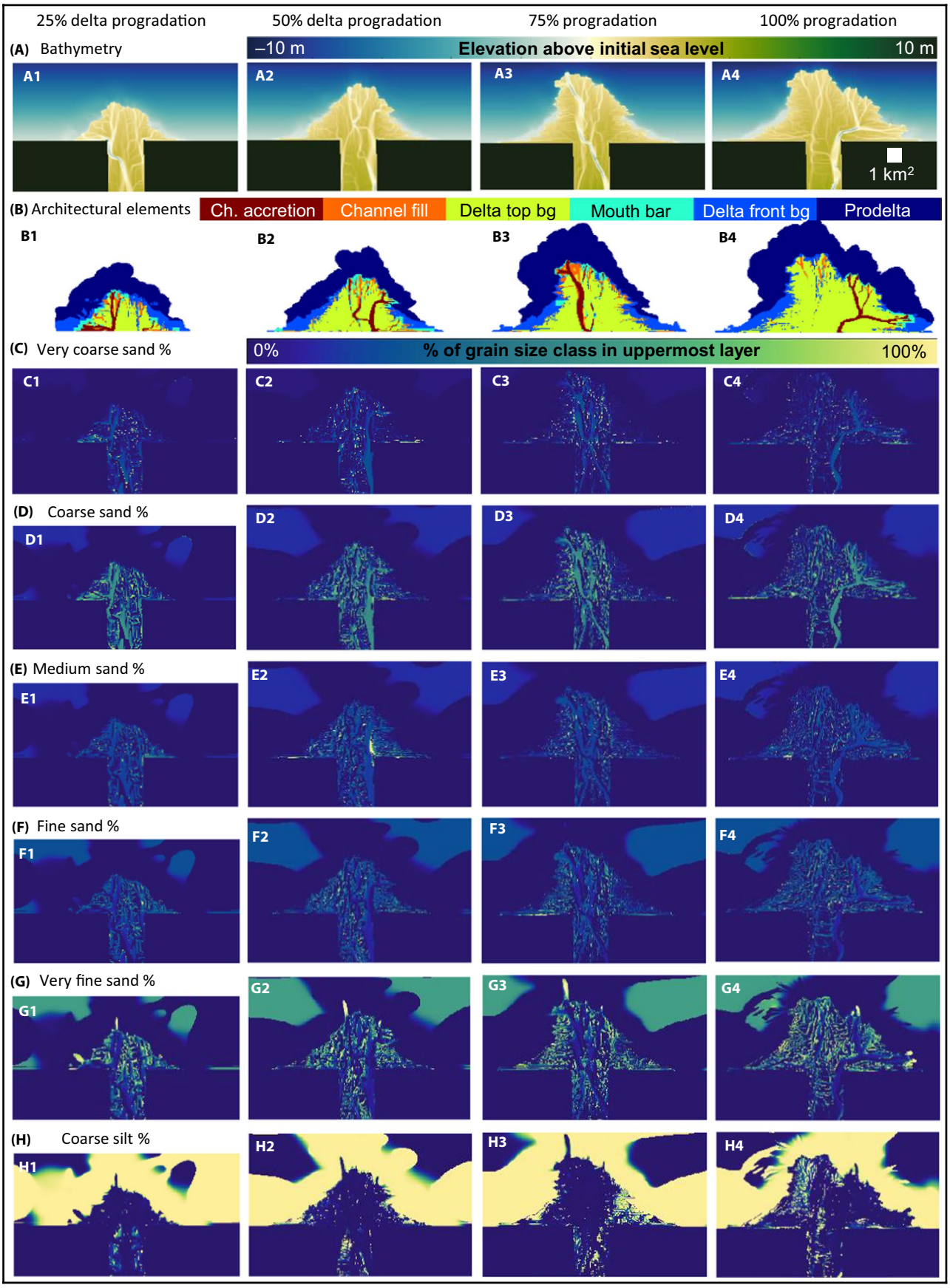

FIGURE 2 For the evolution of the coarse sand delta: (A) bathymetry, (B) distribution of architectural elements, (C–H) distributions of individual grain size classes. The four columns each show snapshots of four stages in the evolution of the delta

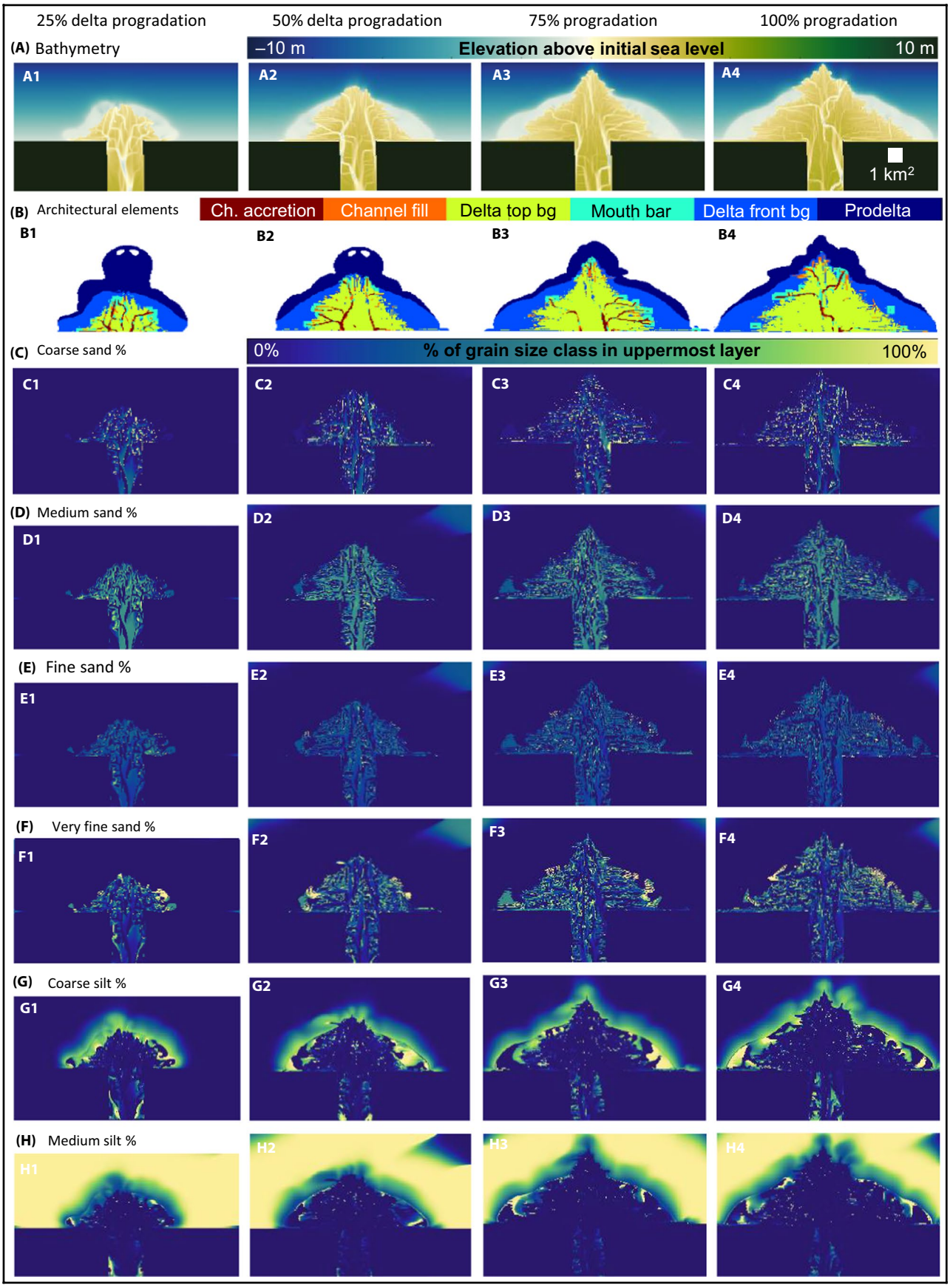

FIGURE 3 For the evolution of the medium sand delta: (A) bathymetry, (B) distribution of architectural elements, (C–H) distributions of individual grain size classes. The four columns each show snapshots of four stages in the evolution of the delta

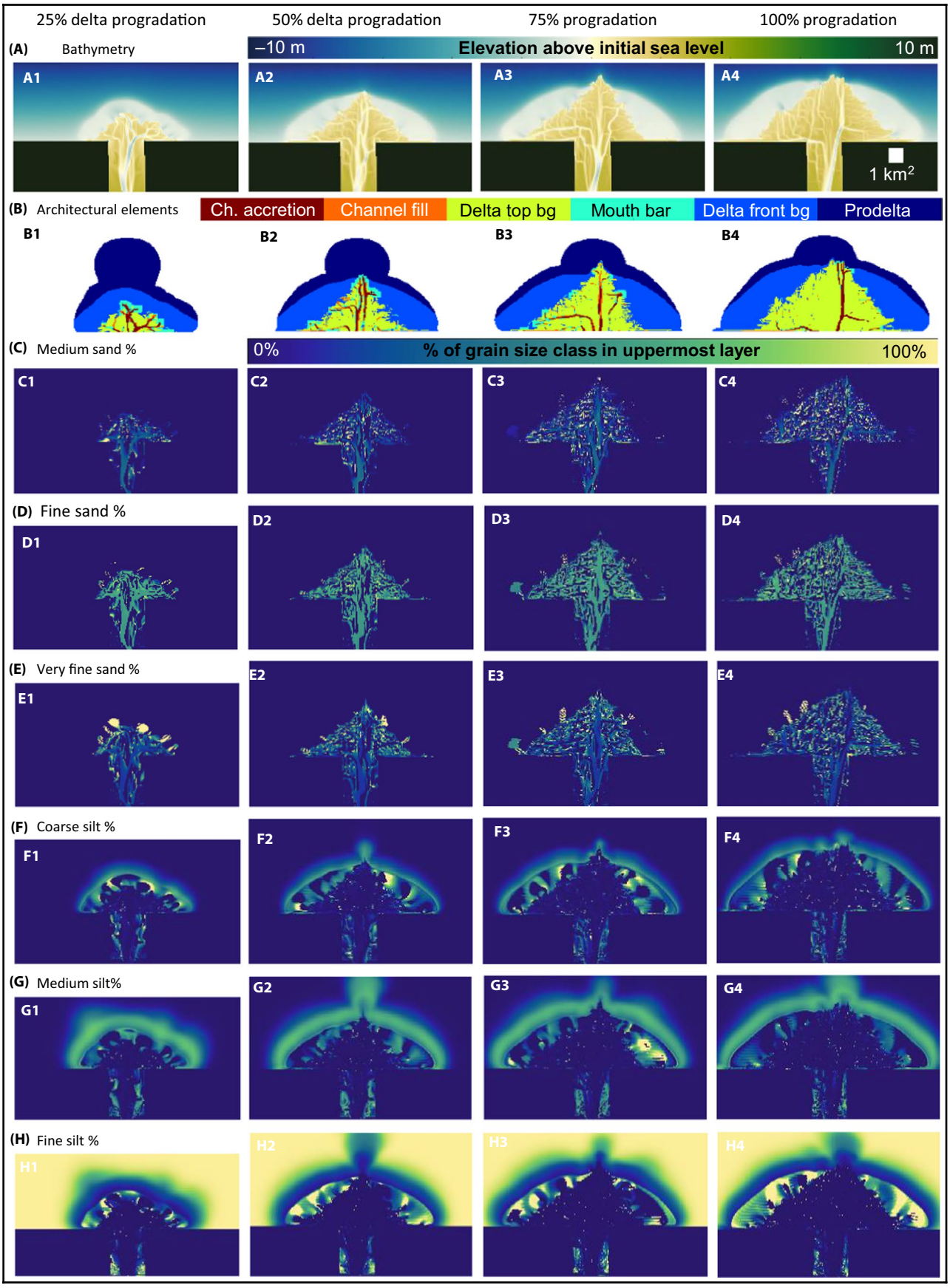

FIGURE 4 For the evolution of the fine sand delta: (A) bathymetry, (B) distribution of architectural elements, (C)-(H) distributions of individual grain size classes. The four columns each show snapshots of four stages in the evolution of the delta

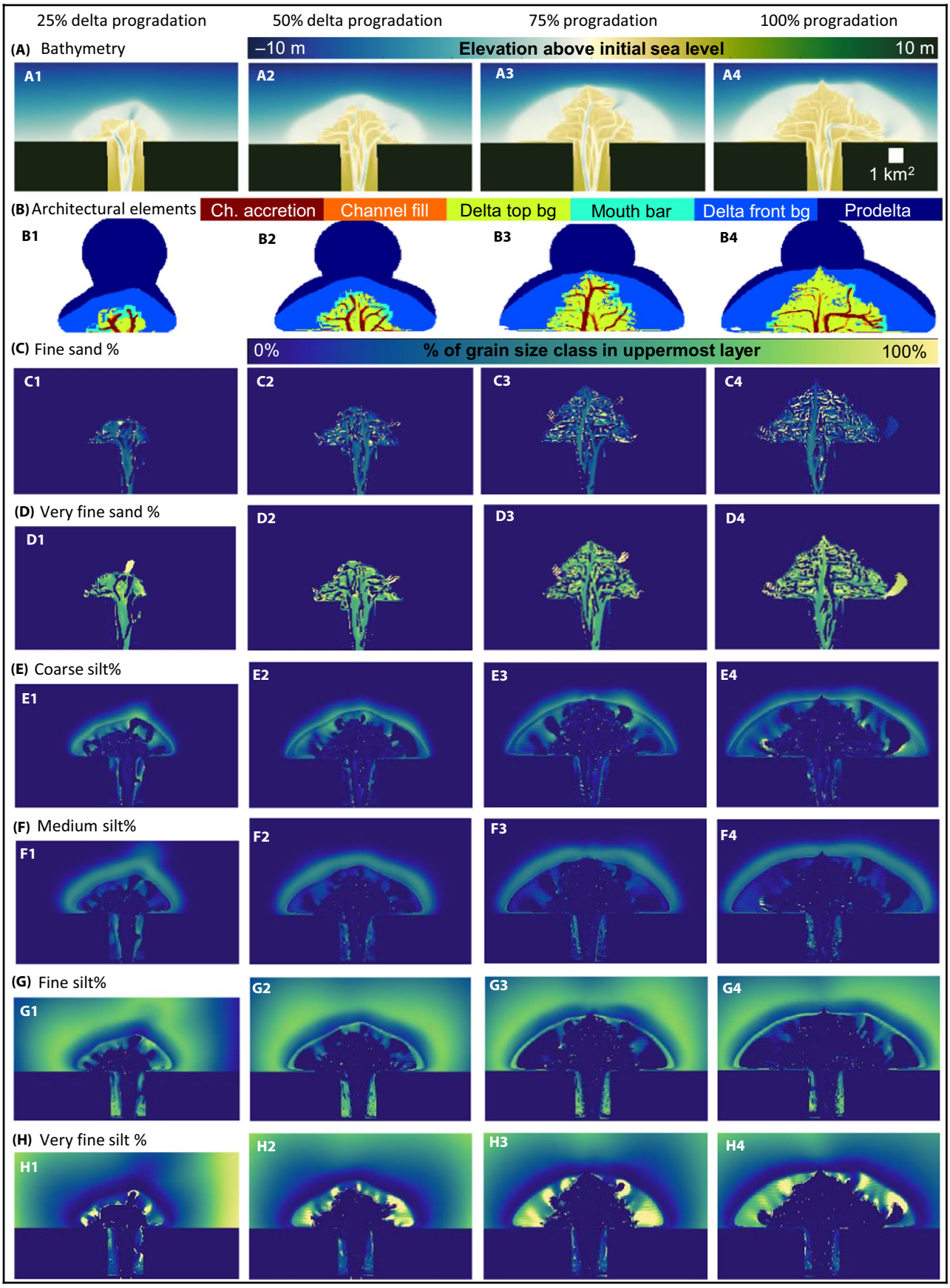

FIGURE 5 For the evolution of the very fine sand delta: (A) bathymetry, (B) distribution of architectural elements, (C–H) distributions of individual grain size classes. The four columns each show snapshots of four stages in the evolution of the delta

figures, as these architectural elements are small in their areal dimensions compared to the delta top background, the delta front background and the prodelta deposits.

The cohesive sediment supplied to the delta (coarse to very fine silt classes) are mainly deposited as delta front and prodelta, or even more distally into the basin. The delta front background sedimentation occurs above the wave base while the prodelta sedimentation occurs below the wave base, therefore the hydrodynamic processes affecting the cohesive sediment fractions also differ for these two architectural elements.

The effects of waves impact background delta front deposition by displacing cohesive sediment further offshore. In addition, the delta front is closer to the channel network, so the interaction between the discharge at the channel mouths and marine processes plays a large role. A good example of depositional trends in the delta front background can be seen in the very fine sand delta (Figure 5E through H). Here very fine silt deposits close to channel mouths, especially when they are shifting or in the process of being abandoned. In contrast, fine silt deposits further away from the channel mouths including at the distal edges of the delta front, where the fine silt fraction can settle just below wave base. The edge of the resulting platform created by the waves provides more vertical space for the fine silt fraction to accumulate, even though the plan view extent of the fine silt fraction seems more confined relative to the very fine silt fraction. Medium and coarse silt fractions deposit in the same locations as the fine silt fraction, but also further from the channel mouths. It may seem counterintuitive that finer grained sediment deposits closer to a high energy channel environment. However, it is important to note that the finer cohesive fractions are not only defined by slower settling velocities, but also by larger critical shear stress for erosion. The same trend can be observed in the other simulated deltas.

The prodelta, deposited below wave base, consists of coarser silts depositing close to the delta front and the finer silts depositing further into the basin. In the very fine sand delta (Figure 5), the distance at which each of the four sediment classes deposits from the boundary of the delta front determines how much will be included in the prodelta. Very fine and fine silt deposits even further into the basin than the prodelta boundary, and thus provides only a small contribution to the prodelta composition. Medium and coarse silt deposits closer to the delta front and therefore makes up a large proportion of the prodelta. The same is true for the fine sand delta (Figure 4), where fine and medium silt dominate prodelta deposition. In the medium sand delta (Figure 3), not only medium silt but also coarse silt accumulates as prodelta deposits, and in the coarse sand delta the majority of the prodelta is comprised of coarse silt. In simulations with coarser sediment supplies, there are not only fewer silt classes available for deposition in the delta front, but the fluvial discharge assigned to the coarser sediment simulations is also larger, allowing sediment with a larger settling velocity to reach the prodelta.

Before further analysing the composition of each architectural element, it is important to address the question: How important is each of the architectural elements within each of the deltas' overall architecture? The plan view maps (Figures 2 through 5) show the large areal extent of some of the architectural elements (e.g. delta top background, delta front background and prodelta), but how does this translate into their importance in the overall deposited mass? To answer this, the percentage each architectural element contributes to the total deposited sediment mass in its delta was calculated (Figure 6). In many cases, the most extensive architectural elements by area constitute less than 5% of the total deposited mass in the delta. This is the case for the channel fill and delta top background in all the deltas. Also the channel accretion in the very fine sand delta and the delta front background and prodelta in the coarse and medium sand deltas constitute less than 5% of the deposited mass in their respective deltas.

It is particularly important to note that in all four of these delta examples, the mouth bar deposits make up the majority of the deposited mass in the delta. Second by mass are the channel accretion deposits, with the delta front deposits also playing an important role in the very fine sand delta's

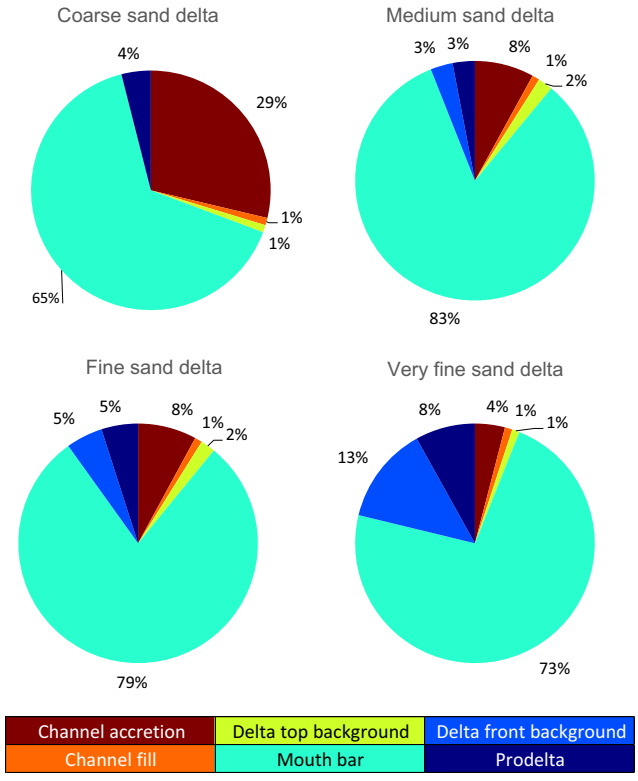

FIGURE 6 Proportion each architectural element contributes to the final delta deposit by sediment mass

architecture. This contrasts with the observation that the mouth bar and channel accretion architectural elements are the least extensive when viewing the plan view maps of the architectural elements (Figures 2 through 5).

The differences in channel accretion deposits between the deltas are related to the differences in lateral mobility of the channel network. In turn, the delta front architecture is also linked to channel network mobility as sediment is delivered to it by the channel network. The greater the lateral mobility of the channel network, the larger the area at the delta front to which sediment is delivered. To understand how the differences in delta architecture relate to channel network mobility, a proxy for channel mobility was calculated for each delta. To this end the percentage of the channel network area that becomes abandoned between simulation output intervals (i.e. the proportion of the channel network that is no longer active when a channel permanently avulses, temporarily avulses or makes a lateral shift) is calculated for each delta, across all output intervals (Figure 7). Not only does the channel mobility decrease from coarser to finer grained sediment supply, but the variability in the channel mobility also decreases. Pronounced deposition is expected within a channel immediately following a large shift in the channel network. Therefore, large values of channel mobility, as well as the spread of the data points, can be at least as important as the mean values exactly because they encapsulate the times at which the largest changes occur.

The geometric mean grain size of the preserved deposit composition for each architectural element was calculated at the end of each simulation in order to compare their overall sediment compositions, both to each other and to the compositions of their respective supplies (Figure 8).

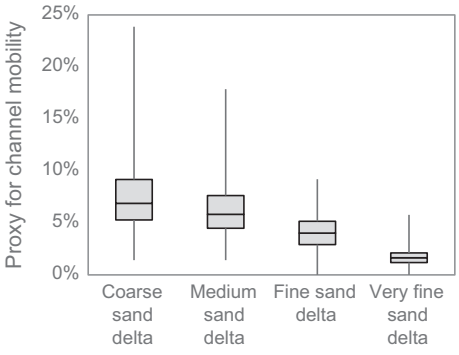

FIGURE 7 The percentage of the channel network area changing from active to inactive between simulation output intervals, serve as a proxy for channel mobility. The larger the proportion of the channel network being abandoned, the more mobile the channel network. The graph shows the mean value (second quartile, horizontal black line) between the first and third quartiles (represented by the grey boxes). The maximum and minimum ranges are indicated by the vertical black lines. All data points throughout the entire simulated interval were used in the calculation

It was assumed that for architectural elements contributing less than 5% to the final deposit it is likely that noise will overprint the trends across such a limited amount of data. Therefore these elements are not discussed further in the trend descriptions. Their geometric mean grain sizes are, however, still included in Figure 8 for the sake of completeness.

Although coarser than the geometric mean of the supply, the geometric mean grain size of the channel accretion deposits decreases proportionally to that of the supply composition. In contrast, the geometric mean grain sizes of the mouth bar deposits of the different deltas are closer together than those of their supplied sediment. While the geometric mean grain size values of the supply compositions span a range of ~250 μm, those of the mouth bar deposits only span a range of ~180 μm. The effect of selective deposition within the architectural elements is even more evident in the delta front background and prodelta, where the geometric mean grain size of these elements only differ by ~15 μm, while the respective supply compositions in the two deltas vary by more than double that, i.e. ~40 μm.

The composition of the channel accretion deposits remains relatively constant within any one delta over the course of the simulated delta evolution (Figure 9A1, B1 and C1). In the final preserved composition, the very coarse sand to fine sand is overrepresented in the channel accretion deposits. The grain size composition of the mouth bars also remains relatively

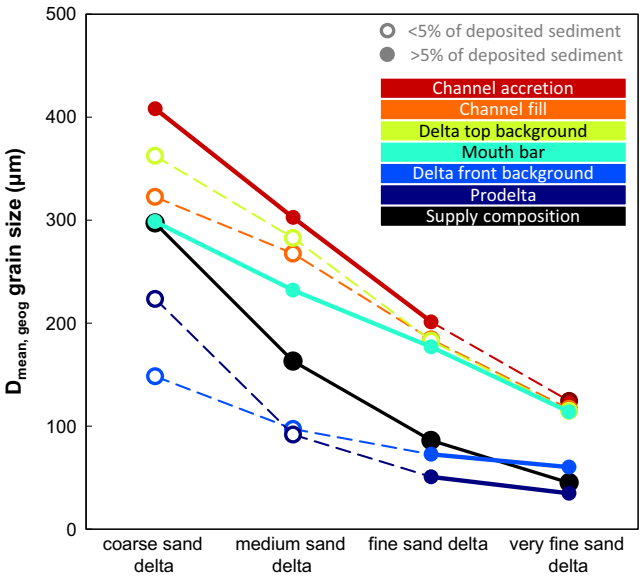

FIGURE 8 The geometric mean grain size of each architectural element for each of the four simulated deltas. Architectural elements which contribute less than 5% of the final mass of the delta are displayed in empty circles with dotted lines. These elements constitute so little of the overall delta sedimentation that their composition may be overprinted by noise and therefore should be considered as secondary data in the trend analysis. The geometric mean of the sediment composition supplied to each delta is also presented in black

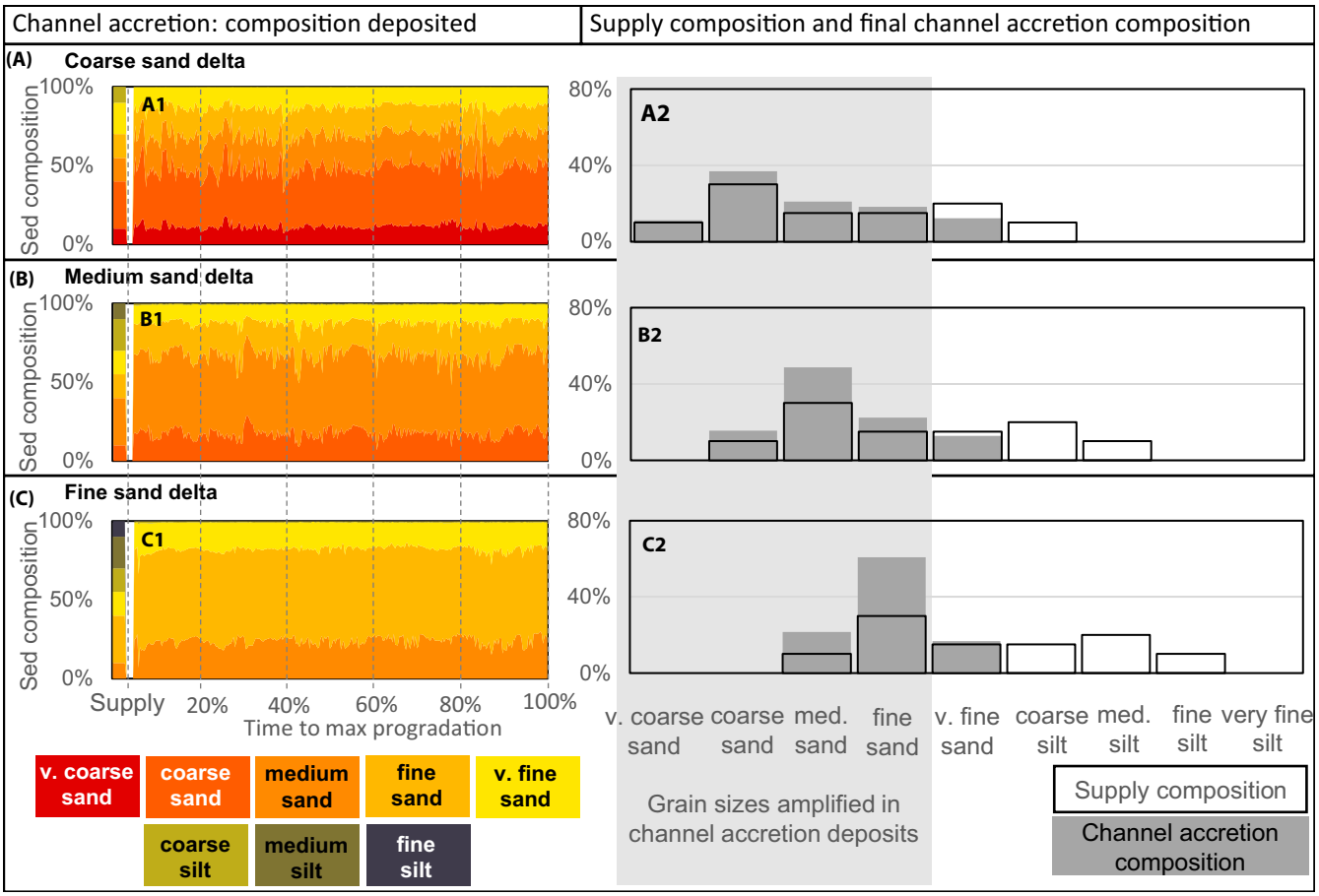

FIGURE 9 The left column shows the composition of the channel accretion deposited in each output time interval for all three simulations where the channel accretion deposits made up more than 5% of the overall deposited sediment. The bar on the left shows the composition of the sediment supplied to the delta. On the right, the final sediment composition of the channel accretion deposits preserved at the end of the simulation is compared to the sediment composition supplied to the delta. Grain size classes very coarse to fine sand occur in a larger proportion in these channel accretion deposits than in the sediment supply for all models. Grain size classes outside of this range are deposited in reduced proportions in the channel accretion deposits

constant within any one delta over the course of the simulation (Figure 10A1, B1, C1 and D1). In the final preserved mouth bar deposit the medium sand to very fine sand is overrepresented. This means that the mouth bar composition, which makes up the majority of the deposited mass of the delta, is even less representative of the sediment supply in muddy deltas than in sandy deltas. The silt fractions present in the supply are significantly diminished in the mouth bar deposits.

In contrast to the constant composition seen in the channel accretion and mouth bar deposits over time, the delta front background deposits show a coarsening over time (Figure 11A1 and B1). At the end of the simulation, the grain size compositions of both the fine sand and very fine sand deltas show an increased proportion of very fine sand to medium silt preserved compared to their supply compositions. However, due to the coarsening trend over time it is not certain that this will remain the case as the delta builds further into the basin, encountering an ever deeper water column. This coarsening over time is also observed, albeit to a lesser extent, in the prodelta deposits (Figure 12A1 and B1). By the end of the simulations there is not a continuous coarsening trend in the prodelta as there is in the delta front background deposits. Instead, the prodelta deposits show episodic sand deposition in the fine sand delta, and also to a lesser extent in the very fine sand delta.

4 | DISCUSSION

This study focusses on the fractionation and preservation of the upstream sediment composition within the architectural elements of deltaic depositional environments. As can be expected (Orton and Reading, 1993), the coarser the sediment supply the more sedimentation occurs closer to the fluvial domain, typically as channel accretion and mouth bar deposits. The finer the sediment supply the more sedimentation occurs further away from the source, e.g. in the delta front background and prodelta.

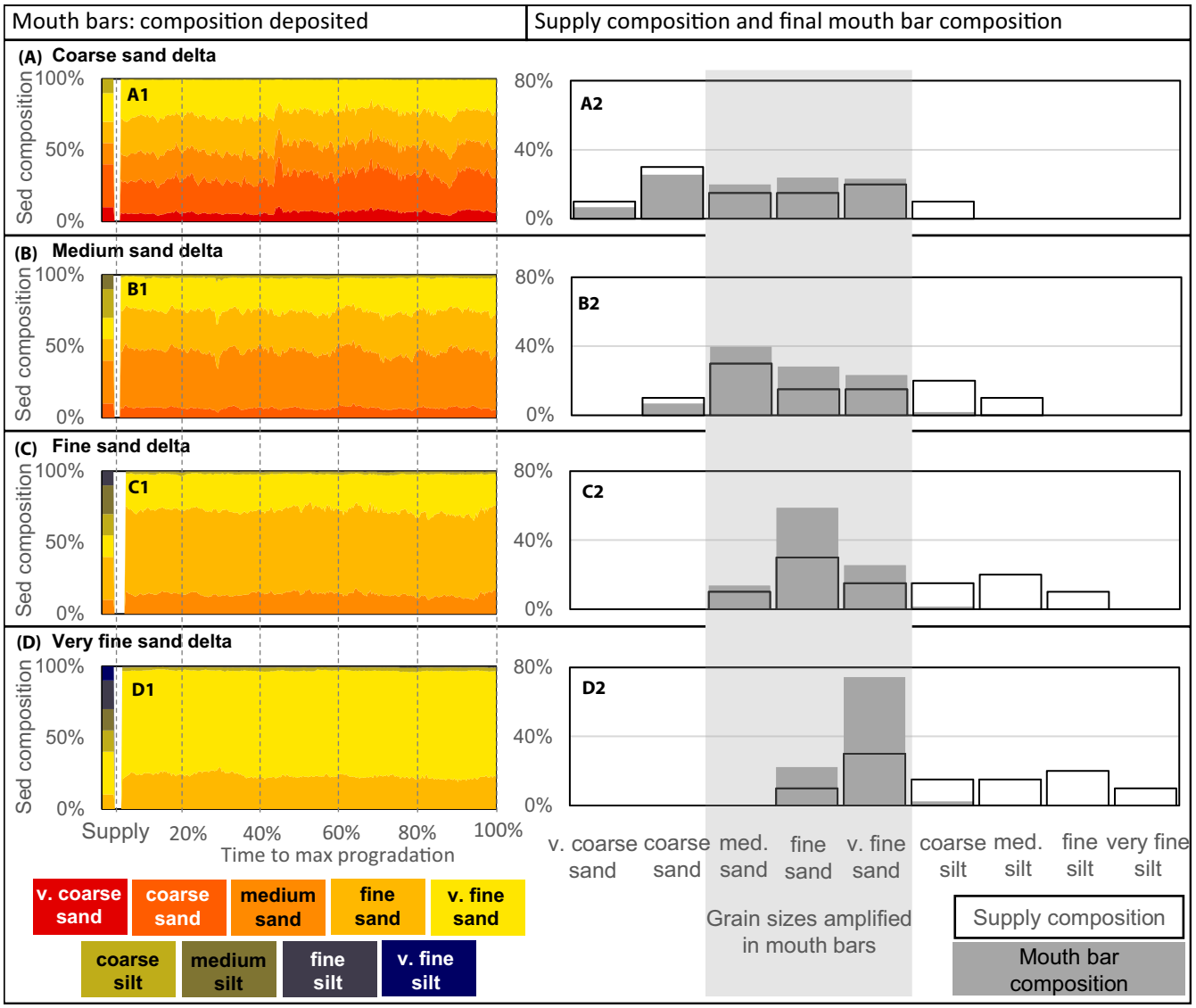

FIGURE 10 The left column shows the composition of the mouth bars deposited in each output time interval for all four simulations. The bar on the left shows the composition of the sediment supplied to the delta. On the right, the final sediment composition of the mouth bar deposits preserved at the end of the simulation is compared to the sediment composition supplied to the delta. Grain size classes medium to very fine sand occur in a larger proportion in these mouth bar deposits than in the sediment supply for all models. Grain size classes outside of this range are deposited in reduced proportions in the mouth bar deposits

The area spanned by each architectural element is found to not be representative of the importance of that element in the final preserved three-dimensional sediment mass constituting the delta. In the simulations, the channel accretion and mouth bar deposits together constitute between 75% (finest grain delta) and 95% (coarsest grained delta) of the delta deposit. However, these two architectural elements only make up a small proportion of the area of the delta plan view at any one time. The mouth bar deposits in particular constitute a large proportion of all the sediment mass that is deposited in the delta. This observation corresponds with literature references labelling these architectural elements as some of the most important in deltaic environments (Reading and Collinson, 1986; Howell *et al.*, 2008).

Very little delta top background deposition is recorded in these simulations. This does not mean that this element is not important in natural systems. There are many examples of preserved un-channelized delta plain deposits (Fielding, 1985; Willis *et al.*, 1999). The potential under-representation of delta top background deposition could also indicate that the processes simulated in these models are not the most important processes responsible for capturing deposition on the delta plain. Processes like vegetation growth, compaction and peat growth, which are currently not included, all contribute to the accumulation of mass on the delta plain. A rising sea level will also create accommodation on the delta top, leading to larger trapping potential of delta top background sedimentation. While floodplain dynamics was not the focus of

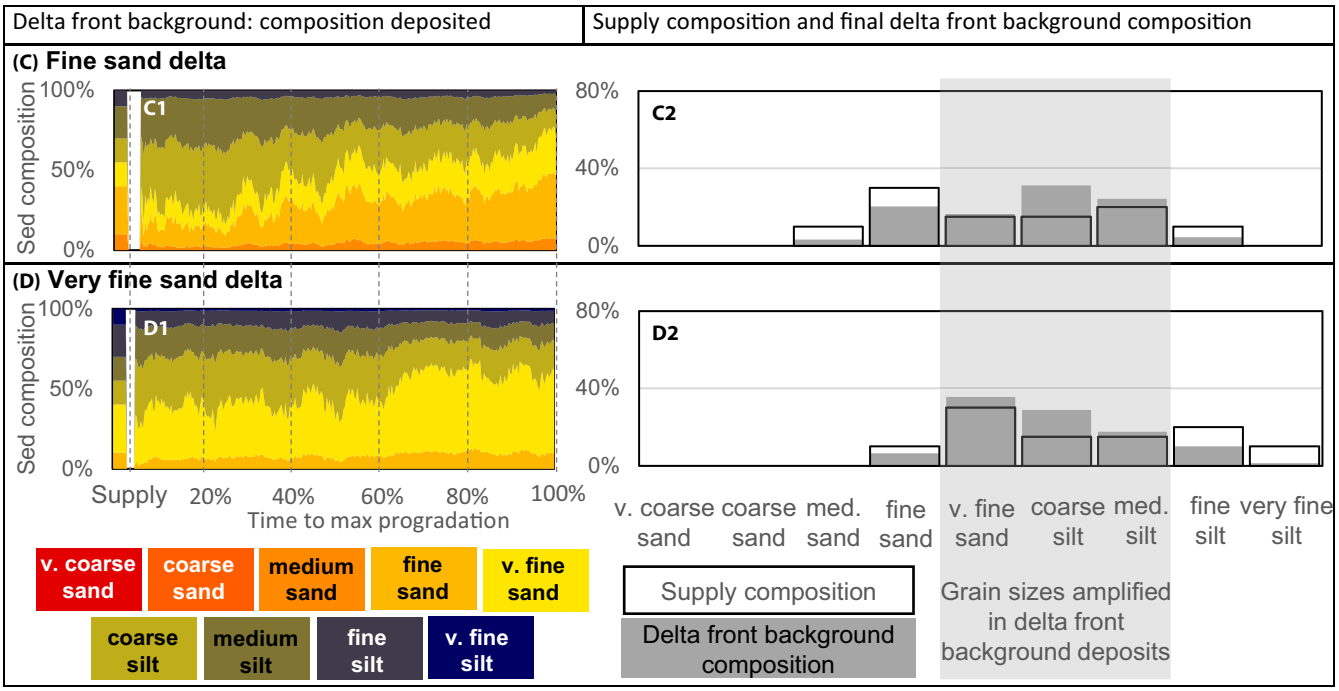

FIGURE 11 The left column shows the composition of the delta front background deposits in each output time interval for the two simulations where this element made up more than 5% of the total deposited sediment. The bar on the left shows the composition of the sediment supplied to the delta. On the right, the final sediment composition of the delta front background composition preserved at the end of the simulation is compared to the sediment composition supplied to the delta. Grain size classes very fine sand to medium silt occur in a larger proportion in these delta front background deposits than in the sediment supply for all models. Grain size classes outside of this range are deposited in reduced proportions in the delta front background deposits

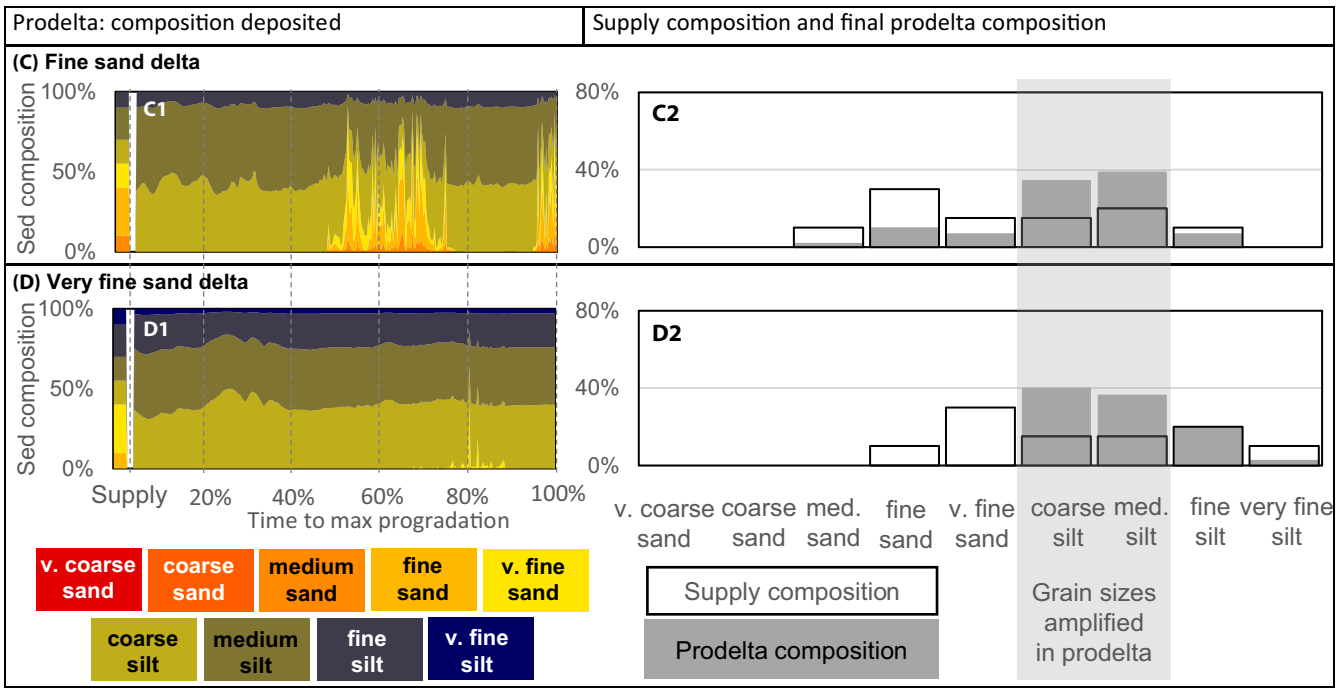

FIGURE 12 The left column shows the composition of the prodelta deposits in each output time interval for the two simulations where this element made up more than 5% of the total deposited sediment. The bar on the left shows the composition of the sediment supplied to the delta. On the right, the final sediment composition of the prodelta composition preserved at the end of the simulation is compared to the sediment composition supplied to the delta. Grain size classes coarse to fine silt occur in a larger proportion in these prodelta deposits than in the sediment supply for all models. Grain size classes outside of this range are deposited in reduced proportions in the prodelta

this study, it could be possible to combine these processes in future studies (Oorschot *et al.*, 2015; Li *et al.*, 2017; Nienhuis *et al.*, 2018).

The disconnect between architectural elements which are important in the plan view snapshots versus those important in the preserved sediment mass is to be expected. Depositional processes which diffuse sediment will typically also lead to thinner, more laterally extensive deposits. In contrast, coarser material which requires high flow velocities to be transported will be less concentrated in areas where the flow is the largest, but therefore also confined to areas in proximity to the channelized features.

This active channel network was found to be more mobile across the delta top in deltas with a coarser sediment supply. Under these conditions, a larger part of the channel network becomes inactive per output time interval as the channels shift laterally. This leads to more channel accretion deposits in the coarser supply deltas. However, this also leads to a feedback mechanism between channel mobility and sediment grain size. Coarser sediment supply, transported as bedload more readily deposits at the channel base, leading to shallower channels and thereby stimulating a more mobile channel network.

Grain size classes very course to fine sand are overrepresented in channel accretion deposits compared to their respective supply composition, across all the simulated deltas. At the same time medium to very fine sand grain size classes are overrepresented in the mouth bar deposits. The degree to which certain grain size classes are overrepresented depends on the transport capacity of the channels delivering sediment to the mouth bars, as well as the efficiency with which the sediment arriving at the mouth bars are reworked or removed by the basin hydrodynamic processes from tides and waves.

The supplied grain size composition determines the availability of sediment classes to be deposited in each architectural element. Sand classes that were supplied in large proportions were also found in large proportions in the channel accretion and mouth bar deposits, which make up the majority of the delta deposits. The geometric mean of the mouth bar deposits, which are stratigraphically the most prolific deposits in these deltas, lie closer together than that of the supplied sediment composition (Figures 13 and 14). The introduced sediments span a range of ~250 μm between simulations, while the mouth bar deposits span a range of only ~180 μm.

The same grain size classes are overrepresented per architectural element, irrespective of the supply composition. The significant differences in preservation of e.g. channel accretion deposits between the coarse sand delta (~29%) and the very fine sand delta (~4%) alludes to the fact that the very fine sand delta probably experiences an under-supply of the grain size classes which preferentially deposit in the channels. This is also supported by the fact the very coarse to fine sand grain size classes are amplified in the channel accretion deposits, of which the very fine sand delta has only 10% in its supply composition. It is then not surprising that this delta only preserves 4% of channel accretion deposits in the final architecture. The grain size classes required to build this element are simply not supplied in large enough proportions to

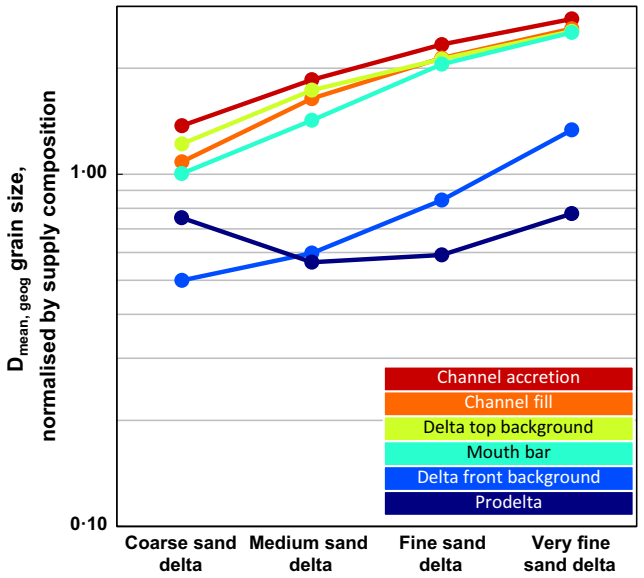

FIGURE 13 The geometric mean of the grain size composition in each architectural element type have been normalised by the supplied sediment composition and plotted on a logarithmic scale. Values larger than 1 indicate coarsening of the composition compared to the supplied composition with larger values indicating more coarsening. Values less than 1 indicate fining compared to the supplied composition

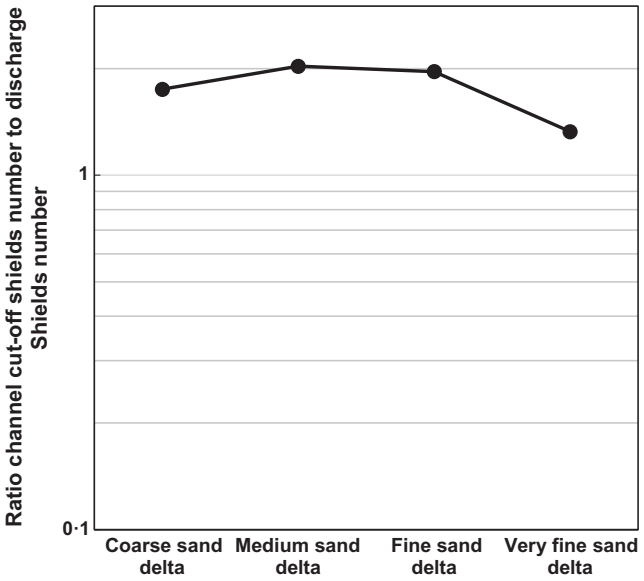

FIGURE 14 The Shields number for the channel recognition cut-off velocity of each of the simulations has been normalised by the Shields number relating to the discharge of that simulation. The resultant curve is very different from any of the normalised coarsening or fining trends seen in the architectural elements in Figure 13 and therefore a linear relationship is unlikely

allow preservation of a larger proportion of channel accretion deposits.

This research therefore suggests that the sediment composition preserved in any architectural element within a delta is not directly proportional to the sediment supply distribution, nor is it fully dependent on sedimentary sorting along the channels or by basinal reworking processes. Instead, a combination of these forces produce a strong process-driven fractionation of sediment grain size classes across the delta, whereby e.g. medium to very fine sand deposition is likely to be overrepresented in mouth bar complexes in both coarse and fine grained deltas. It is not suggested that medium to very fine sand classes will be preferentially preserved in the mouth bars in all natural systems. In deltaic systems where storms and floods dominate deposition, often simultaneously, or where the sediment source area is close by, very course grained mouth bar complexes would still be expected. A good example of such a system would be the Dorothea Formation in the Magallanes Basin in Chile (Hubbard *et al.*, 2010).

Mouth bar complexes, which are defining features in delta architecture and description in the field (Forzoni *et al.*, 2015), show a bias for preserving the sand fractions of the supplied sediment. Simulations reported here show that the preferential preservation and/or description of mouth bars would lead to a biased interpretation of ancient deltaic systems as having a sand-dominated supply. Where muddy clinoforms are described in the literature, they typically refer to shelf formation distal to the delta itself, rather than delta front deposition (Kuehl *et al.*, 2005; Cattaneo *et al.*, 2007). In fact, even in modern deltas which have been classified as muddy/silty based on their supply composition, mouth bar deposits typically remain sandy e.g. the Mississippi (Esposito *et al.*, 2013), Ganges-Brahmaputra (Goodbred *et al.*, 2003), Huange (Li *et al.*, 1998), Mahakam (Storms *et al.*, 2005). In natural systems the occurrence of muddy mouth bar clinoforms are even more unlikely in the presence of marine energy. Even small waves will stir up and remove silt-sized sediment from the mouth bars clinoforms over time. However, tides can cause the formation of mud drapes, which can vary in character based on the asymmetry of the tidal signal. But even under these conditions, the majority of mouth bars in natural systems will still consist of sand rather than mud (Reading and Collinson, 1986).

Some prodeltaic mud beds in the Dunvegan Formation (Alberta, Canada) and the Ferron sandstone Member (Mancos Shale Formation, UT, USA), can be linked to storms, but also to fluvial flooding events (Bhattacharya and MacEachern, 2009). This also implies that the cohesive material deposited in the prodeltas are syn-depositional to the more proximal sandy deposits and should be accounted for when the sediment supply composition of these systems are estimated. Outcrop-based field studies there need to consider how representative sandy mouth bar complexes are of the overall sediment supply composition at any one time. The study of prodelta deposits corresponding to sandy delta front deposits can provide valuable clues to help reconstruct the original sediment supply composition of a system. This paper shows that the majority of fine-grained sediments are deposited as background sedimentation in the delta front and the prodelta. Therefore, whenever distal deposits are not included in sediment reconstructions, the contribution of cohesive sediments are likely to be underestimated. This may have significant implications on the inferred delta shape, morphology, and channel characteristics.

If the supplied sediment is finer, more cohesive, or more likely to be transported in suspension, the individual lobes can be more elongate leading to a rugose shoreline, deposited by a few, deep, stable channels. In contrast if sediment supply is coarser, less cohesive or more likely to travel as bedload, the delta geometry will be more semi-circular with a smoother shoreline, deposited by a mobile network of multiple, shallow channels (Orton and Reading, 1993; Caldwell and Edmonds, 2014; Burpee *et al.*, 2015; van der Vegt *et al.*, 2016). Therefore biases in sediment supply reconstruction, e.g. as overly sandy, could also lead to errors in the inferred geometry/morphologies and ultimately errors in the predictions of facies distribution in the subsurface.

As shown in this study, such bias can be reduced by including the chronostratigraphically related distal/prodelta deposits when studying ancient deltaic systems. A combined description of sandy delta front and delta top, together with the finer-grained delta slope and prodelta deposits provides a more complete understanding of the sediment supply at the time of deposition.

The set of numerical experiments reported here assume sustained input parameters—no changes in discharge, tidal signal or wave regime during the simulation. In natural systems, however, sediment sorting along the sedimentary system is even more complex due to the non-linear responses to time-varying sediment supply, basin reworking processes and base-level fluctuations (Jerolmack and Paola, 2010; Armitage *et al.*, 2011). It is known that short-lived sediment fluctuations may be dampened as they travel through the system, while sustained supply changes are still likely to reach the shallow marine and marine domains (Van Den Berg Van Saparoea and Postma, 2008). In addition, the latest research shows a more complex relationship between the magnitude and duration of the supply signal and ability of the sediment routing system to record this signal (Toby *et al.*, 2019). The findings reported here highlight an additional uncertainty, in that even under idealised, time-constant conditions the source grain size composition may be distorted in the preserved deposits at any single location.

The numerical analogue methodology described here can be applied to test hypotheses on sand body geometry in field

studies for systems where outcrops may not be available. But more generally, statistical study across an extensive database of synthetic and natural delta analogues containing both source and sink information would relate detailed grain size trends to palaeo-conditions and depositional geometries. While source-to-sink studies are imperative to understanding the development of sedimentary systems, detailed unravelling of downstream fining and sorting mechanisms should be a prerequisite for palaeo-environment reconstruction from preserved deposits.

5 | CONCLUSIONS AND IMPLICATIONS

Numerical simulations of delta deposition show that surface observations of actively prograding deltas are not necessarily indicative of the preserved sediment compositions in the subsurface. Some architectural elements, typically those depositing into a deeper water column, make a larger contribution to the preserved deposits than their horizontal extent may suggest. In the simulations reported here, mouth bar complexes constitute the majority of the preserved sediment mass in the delta environment.

The simulations also show to what extent the relative proportions of each architectural element depend on the composition of the supplied sediment. Processes influencing deposition of each architectural element type lead to an overrepresentation of "preferred" grain size classes for that element type. If a supply composition does not contain enough of these "preferred" grain size classes, the corresponding architectural element(s) are undersupplied and likely to constitute a smaller proportion of the final delta deposition. E.g. in simulations where smaller proportions of medium to very fine sand is supplied, the mouth bar deposits constitute a smaller proportion of the overall delta architecture since these grain size classes are typically overrepresented in the mouth bar deposits. The availability of the coarsest grain size classes not only determines the composition and preservation potential of the channel accretion deposits, but also influences the mobility of the channel network and therefore the shape of the delta.

Accounting for these overrepresentations of certain grain size classes in sand-rich architectural elements is imperative in estimates of palaeo-sediment supply from outcrop studies. Accurate palaeo-sediment supply estimates in turn can guide assumptions on delta shape, morphology, and channel characteristics inferred from these studies. Therefore, to constrain the supply composition of a studied system, the syn-depositional, finer, distal deposits in the prodelta should be included in field study analysis where possible.

However, in many ancient delta deposits it may not be possible to quantitatively link thin laterally extending prodeltaic deposits to their corresponding sandy deposits in the field. In these situation, using numerical analogues as proxies to test hypotheses about sediment supply and delta geometries can offer a valuable alternative.

ACKNOWLEDGEMENTS

The authors would like to thank the reviewers Prof Gary Hampson and Prof Maarten Kleinhans for their constructive comments and advice which helped to improve the manuscript. We would also like to thanks Dr. Bert Jagers for answering the many detailed queries on the inner workings of Delft3D.

CONFLICT OF INTEREST

The authors declare no conflicts of interest.

DATA AVAILABILITY STATEMENT

Simulation input, output and post-processed data used in this study can be freely accessed at: https://data.4tu.nl/repository/uuid:8499763f-99e0-4df2-9f53-ff1c30572aae.

ORCID

Helena Vegt https://orcid.org/0000-0003-0506-8744

REFERENCES

Ainsworth, R.B., Vakarelov, B.K., MacEachern, J.A., Nanson, R.A., Lane, T.I., Rarity, F. *et al.* (2016) Process-driven architectural variability in mouth-bar deposits: a case study from a mixed-process mouth-bar complex, Drumheller, Alberta, Canada. *Journal of Sedimentary Research*, *86*(5), 512–541. https://doi.org/10.2110/jsr.2016.23.

Allen, P.A. (2017) *Sediment Routing Systems*. Cambridge, UK: Cambridge University Press. https://doi.org/10.1017/9781316135754.

Armitage, J.J., Duller, R.A., Whittaker, A.C. and Allen, P.A. (2011) Transformation of tectonic and climatic signals from source to sedimentary archive. *Nature Geoscience*, *4*(4), 231–235. https://doi.org/10.1038/ngeo1087.

Bhattacharya, J.P. and MacEachern, J.A. (2009) Hyperpycnal rivers and prodeltaic shelves in the cretaceous seaway of North America. *Journal of Sedimentary Research*, *79*(4), 184–209. https://doi.org/10.2110/jsr.2009.026.

Bhattacharya, J.P., Copeland, P., Lawton, T.F. and Holbrook, J.M. (2016) Estimation of source area, river paleo-discharge, paleoslope, and sediment budgets of linked deep-time depositional systems and implications for hydrocarbon potential. *Earth-Science Reviews*, *153*, 77–110. https://doi.org/10.1016/j.earscirev.2015.10.013.

Burpee, A.P., Slingerland, R.L., Edmonds, D.A., Parsons, D., Best, J., Cederberg, J.A. *et al.* (2015) Grain-size controls on the morphology and internal geometry of river-dominated deltas. *Journal of Sedimentary Research*, *85*(6), 699–714. https://doi.org/10.2110/jsr.2015.39.

Caldwell, R.L. and Edmonds, D.A. (2014) The effects of sediment properties on deltaic processes and morphologies: A numerical modeling study. *Journal of Geophysical Research: Earth Surface*, *119*(5), 961–982. https://doi.org/10.1002/2013JF002965.

Canestrelli, A., Nardin, W., Edmonds, D.A., Fagherazzi, S. and Slingerland, R.L. (2014) Importance of frictional effects and jet instability on the morphodynamics of river mouth bars and levees. *Journal of Geophysical Research: Oceans*, *119*(1), 509–522. https://doi.org/10.1002/2013JC009312.

Cattaneo, A., Trincardi, F., Asioli, A. and Correggiari, A. (2007) The Western Adriatic shelf clinoform: energy-limited bottom-set. *Continental Shelf Research*, *27*(3–4), 506–525. https://doi.org/10.1016/j.csr.2006.11.013.

Edmonds, D.A. and Slingerland, R.L. (2007) Mechanics of river mouth bar formation: implications for the morphodynamics of delta distributary networks. *Journal of Geophysical Research*, *112*(F2), F02034. https://doi.org/10.1029/2006JF000574.

Edmonds, D.A. and Slingerland, R.L. (2009) Significant effect of sediment cohesion on delta morphology. *Nature Geoscience*, *3*(2), 105–109. https://doi.org/10.1038/ngeo730.

Esposito, C.R., Georgiou, I.Y. and Kolker, A.S. (2013) Hydrodynamic and geomorphic controls on mouth bar evolution. *Geophysical Research Letters*, *40*(8), 1540–1545. https://doi.org/10.1002/grl.50333.

Fielding, C.R. (1985) Coal depositional models and the distinction between alluvial and delta plain environments. *Sedimentary Geology*, *42*(1–2), 41–48. https://doi.org/10.1016/0037-0738(85)90072-7.

Forzoni, A., Hampson, G.J. and Storms, J.E.A. (2015) Along-Strike variations in stratigraphic architecture of shallow-marine reservoir analogues: Upper cretaceous Panther Tongue delta and coeval shoreface, Star Point Sandstone, Wasatch Plateau, Central Utah, U.S.A. *Journal of Sedimentary Research*, *85*(8), 968–989. https://doi.org/10.2110/jsr.2015.69.

Gao, W., Shao, D., Wang, Z.B., Nardin, W., Yang, W., Sun, T. *et al.* (2019) Combined effects of unsteady river discharges and wave conditions on river mouth bar morphodynamics. *Geophysical Reserach Letters*, *45*(23), 12903–12911. https://doi.org/10.1029/2018GL080447.

Geleynse, N., Storms, J.E.A., Stive, M.J.F., Jagers, H.R.A. and Walstra, D.J.R. (2010) Modeling of a mixed-load fluvio-deltaic system. *Geophysical Research Letters*, *37*(5), 1–7. https://doi.org/10.1029/2009GL042000.

Goodbred, S.L., Kuehl, S.A., Steckler, M.S. and Sarker, M.H. (2003) Controls on facies distribution and stratigraphic preservation in the Ganges-Brahmaputra delta sequence. *Sedimentary Geology*, *155*(3–4), 301–316. https://doi.org/10.1016/S0037-0738(02)00184-7.

Helland-Hansen, W., Sømme, T.O., Martinsen, O.J., Lunt, I. and Thurmond, J. (2016) Deciphering Earth's natural hourglasses: perspectives on source-to-sink analysis. *Journal of Sedimentary Research*, *86*(September), 1008–1033. https://doi.org/10.2110/jsr.2016.56.

Howell, J.A., Skorstad, A., MacDonald, A., Fordham, A., Flint, S., Fjellvoll, B. *et al.* (2008) Sedimentological parameterization of shallow-marine reservoirs. *Petroleum Geoscience*, *14*(1), 17–34. https://doi.org/10.1144/1354-079307-787.

Hubbard, S.M., Fildani, A., Romans, B.W., Covault, J.A. and McHargue, T.R. (2010) High-Relief Slope Clinoform Development: Insights from Outcrop, Magallanes Basin, Chile. *Journal of Sedimentary Research*, *80*(5), 357–375. https://doi.org/10.2110/jsr.2010.042.

Jerolmack, D.J. and Paola, C. (2010) Shredding of environmental signals by sediment transport. *Geophysical Research Letters*, *37*(October), 1–5. https://doi.org/10.1029/2010GL044638.

Jimenez-Robles, A.M., Ortega-Sanchez, M. and Losada, M.A. (2016) Effects of basin bottom slope on jet hydrodynamics and river mouth bar formation. *Journal of Geophysical Research F: Earth Surface*, *121*(6), 1110–1133. https://doi.org/10.1002/2016JF003871.

Kuehl, S.A., Allison, M.A., Goodbred, S.L., Kudrass, H. (2005) The Ganges-Brahmaputra delta. In Giosan, L., Bhattacharya, J.P. (ed) *River Deltas–Concepts, Models, and Examples*. Tulsa, USA: SEPM Special Publication, *83*, pp. 413–434.

Leonardi, N., Canestrelli, A., Sun, T. and Fagherazzi, S. (2013) Effect of tides on mouth bar morphology and hydrodynamics. *Journal of Geophysical Research: Oceans*, *118*(9), 4169–4183. https://doi.org/10.1002/jgrc.20302.

Lesser, G.R., Roelvink, D.J.A., van Kester, J.A.T.M. and Stelling, G.S. (2004) Development and validation of a three-dimensional morphological model. *Coastal Engineering*, *51*(8–9), 883–915. https://doi.org/10.1016/j.coastaleng.2004.07.014.

Li, G., Wei, H., Yue, S., Cheng, Y. and Han, Y. (1998) Sedimentation in the Yellow River delta, Part II: suspended sediment dispersal and deposition on the subaqueous delta. *Marine Geology*, *149*(1–4), 113–131. https://doi.org/10.1016/S0025-3227(98)00032-2.

Li, L., Storms, J.E.A. and Walstra, D.J.R. (2017) On the upscaling of process-based models in deltaic applications. *Geomorphology*, *304*, 201–213. https://doi.org/10.1016/j.geomorph.2017.10.015.

Mariotti, G., Falcini, F., Geleynse, N., Guala, M., Sun, T. and Fagherazzi, S. (2013) Sediment eddy diffusivity in meandering turbulent jets: Implications for levee formation at river mouths. *Journal of Geophysical Research: Earth Surface*, *118*(3), 1908–1920. https://doi.org/10.1002/jgrf.20134.

Michael, N.A., Whittaker, A.C., Carter, A. and Allen, P.A. (2014) Volumetric budget and grain-size fractionation of a geological sediment routing system: eocene Escanilla Formation, south-central Pyrenees. *Bulletin of the Geological Society of America*, *126*(3–4), 585–599. https://doi.org/10.1130/B30954.1.

Milliman, J.D. and Syvitski, J.P.M. (1992) Geomorphic/tectonic control of sediment discharge to the ocean: the importance of small mountainous rivers. *Journal of Geology*, *100*(5), 525–544.

Nienhuis, J.H., Törnqvist, T.E. and Esposito, C.R. (2018) Crevasse splays versus avulsions: a recipe for land building with levee breaches. *Geophysical Research Letters*, *45*(9), 4058–4067, https://doi.org/https://doi.org/10.1029/2018GL077933 .

van Oorschot, M., Kleinhans, M., Geerling, G. and Middelkoop, H. (2015) Distinct patterns of interaction between vegetation and morphodynamics. *Earth Surface Processess and Landforms*, *41*(6), 791–808. https://doi.org/10.1002/esp.3864

Orton, G.J. and Reading, H.G. (1993) Variability of deltaic processes in terms of sediment supply, with particular emphasis on grain size. *Sedimentology*, *40*, 475–512. https://doi.org/10.1111/j.1365-3091.1993.tb01347.x.

Reading, H.G. and Collinson, J.D. (1986) Clastic coasts. In: Reading, H.G. (Ed.) *Sedimentary Environments: Processes, Facies and Stratigraphy*. Oxford: Blackwell Science.

Storms, J.E.A., Hoogendoorn, R.M., Dam, R.A.C., Hoitink, A.J.F. and Kroonenberg, S.B. (2005) Late-Holocene evolution of the Mahakam delta, East Kalimantan, Indonesia. *Sedimentary Geology*, *180*(3–4), 149–166. https://doi.org/10.1016/j.sedgeo.2005.08.003.

Storms, J.E.A., Stive, M.J.F., Roelvink, D.J.A. and Walstra, D.J.R. (2007) Initial morphologic and stratigraphic delta evolution related to buoyant river plumes. In: Kraus, N.C. and Rosati, J.D. (Eds.) *Sixth International Symposium on Coastal Engineering and Science of Coastal Sediment Processes* (vol. 40926, pp. 736–748). New Orleans, LA. http://dx.doi.org/10.1061/40926(239)56.

Syvitski, J.P.M. and Farrow, G.E. (1989) Fjord sedimentation as an analogue for small hydrocarbon-bearing fan deltas. *Geological Society, London, Special Publications*, *41*(1), 21–43.

Syvitski, J.P.M. and Saito, Y. (2007) Morphodynamics of deltas under the influence of humans. *Global and Planetary Change*, *57*(3–4), 261–282. https://doi.org/10.1016/j.gloplacha.2006.12.001.

Syvitski, J.P.M., Kettner, A.J., Correggiari, A. and Nelson, B.W. (2005) Distributary channels and their impact on sediment dispersal. *Marine Geology*, *222–223*(1–4), 75–94. https://doi.org/10.1016/j.margeo.2005.06.030.

Toby, S.C., Duller, R.A., De Angelis, S. and Straub, K.M. (2019) A stratigraphic framework for the preservation and shredding of environmental signals. *Geophysical Research Letters*. in press, https://doi.org/10.1029/2019GL082555.

Van Den Berg Van Saparoea, A.-P.H. and Postma, G. (2008) Control of climate change on the yield of river systems. *Recent Advances in Models of Siliciclastic Shallow-Marine Stratigraphy*, *90*(90), 1–26. https://doi.org/10.2110/pec.08.90.

van der Vegt, H. (2018) From fluvial supply to delta deposits. Delft University of Technology. https://doi.org/10.4233/uuid:c049ea67-23a1-4e7e-af52-1275802839f1

van der Vegt, H., Storms, J.E.A., Walstra, D.J.R. and Howes, N.C. (2016) Can bed load transport drive varying depositional behaviour in river delta environments? *Sedimentary Geology*, *345*, 19–32. https://doi.org/10.1016/j.sedgeo.2016.08.009.

Willis, B.J., Bhattacharya, J.P., Gabel, S.L. and White, C.D. (1999) Architecture of a tide-induced river delta in the Frontier Formation of central Wyoming, USA. *Sedimentology*, *46*, 667–688.

Wright, L.D. (1977) Sediment transport and deposition at river mouths: a synthesis sediment transport and deposition at river mouths. *Geological Society of America Bulletin*, *88*(6), 857–868. https://doi.org/10.1130/0016-7606(1977)88<857.

How to cite this article: van der Vegt H, Storms JEA, Walstra D-JR, Nordahl K, Howes NC, Martinius AW. Grain size fractionation by process-driven sorting in sandy to muddy deltas. *Depositional Rec*. 2020;6: 217–235. https://doi.org/10.1002/dep2.85

APPENDIX 1

In Figure 13, the geometric mean grain size of each architectural element has been normalized by the geometric mean of the sediment supply composition for that simulation. Values larger than 1 therefore show sediment coarsening compared to the supply composition while values smaller than one show sediment fining compared to the supply composition. In addition, in Figure 14 the Shields number related to each simulations channel cut-off velocity has been normalized by the characteristic Shields number related to its discharge boundary. Based on the shape of these curves it is possible to conclude that there is not an obvious dependency between the selection of the input or analyses parameters and the results of sediment coarsening and fining observed in the architectural elements.